Supplementary Information File

Single-cell analysis of Ribonucleotide reductase (RNR) transcriptional and translational response to DNA damage

Aprotim Mazumder[a], Katja Tummler[a], Mark Bathe[a,#], Leona D. Samson[a,b,#]

[a] Department of Biological Engineering and Center for Environmental Health Sciences, [b] Department of Biology, Massachusetts Institute of Technology, Cambridge, MA 02139, USA

[#] To whom correspondence should be addressed: lsamson@mit.edu; mark.bathe@mit.edu

A

```
RNR1 : 1    atgtacgtttataaaagagacggtcgtaaagaacctgtccaattcgataagattaccgct 60
            |||||||||  ||||||||||||| || ||||| || || |||||||||||| |||||| |
RNR3 : 1    atgtacgttattaaaagagaggccgcaaagagcccgttcaattcgataaaattacctcc 60

RNR1 : 61   cgtatatcacgcttatgctatggtttagatccaaaacatatcgacgccgttaaggtcacc 120
            |||||  | || || |  || |||||||| ||||| | ||| || || |||||||| |||
RNR3 : 61   cgtatcacccgtttgtcatacggtttagacccaaaccgtattgatgctgttaaggtaacc 120

RNR1 : 121  caacgtatcatttctggtgtctatgaaggtgtcacaacaatcgaactagacaacttagcc 180
            |||||||| |||||||||||  ||    ||||| || ||  | || || |||||  | ||
RNR3 : 121  caacgtattatttctggtgtgtactccggtgttactaccgttgagctggacaatcttgca 180 …
```

B

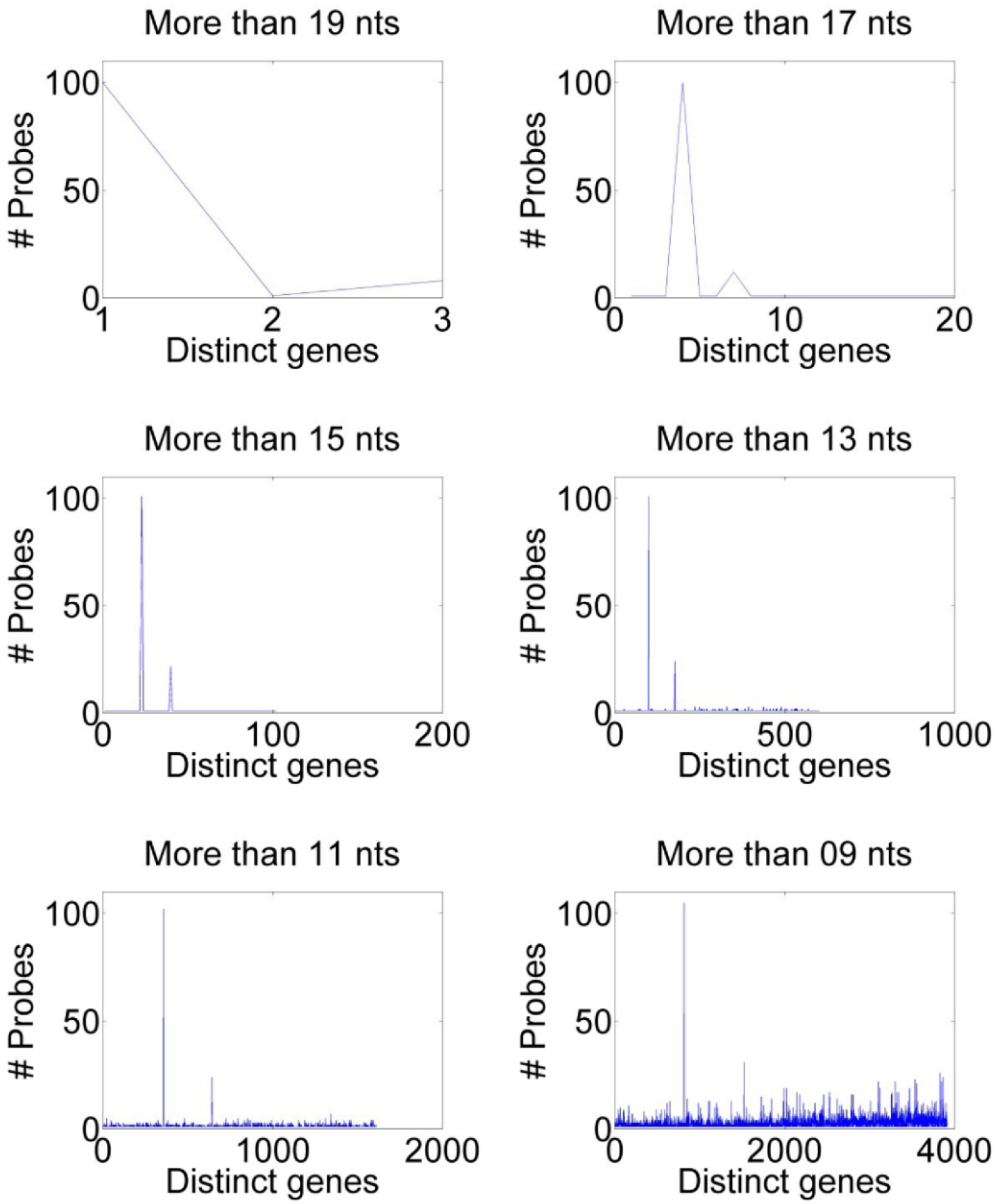

C

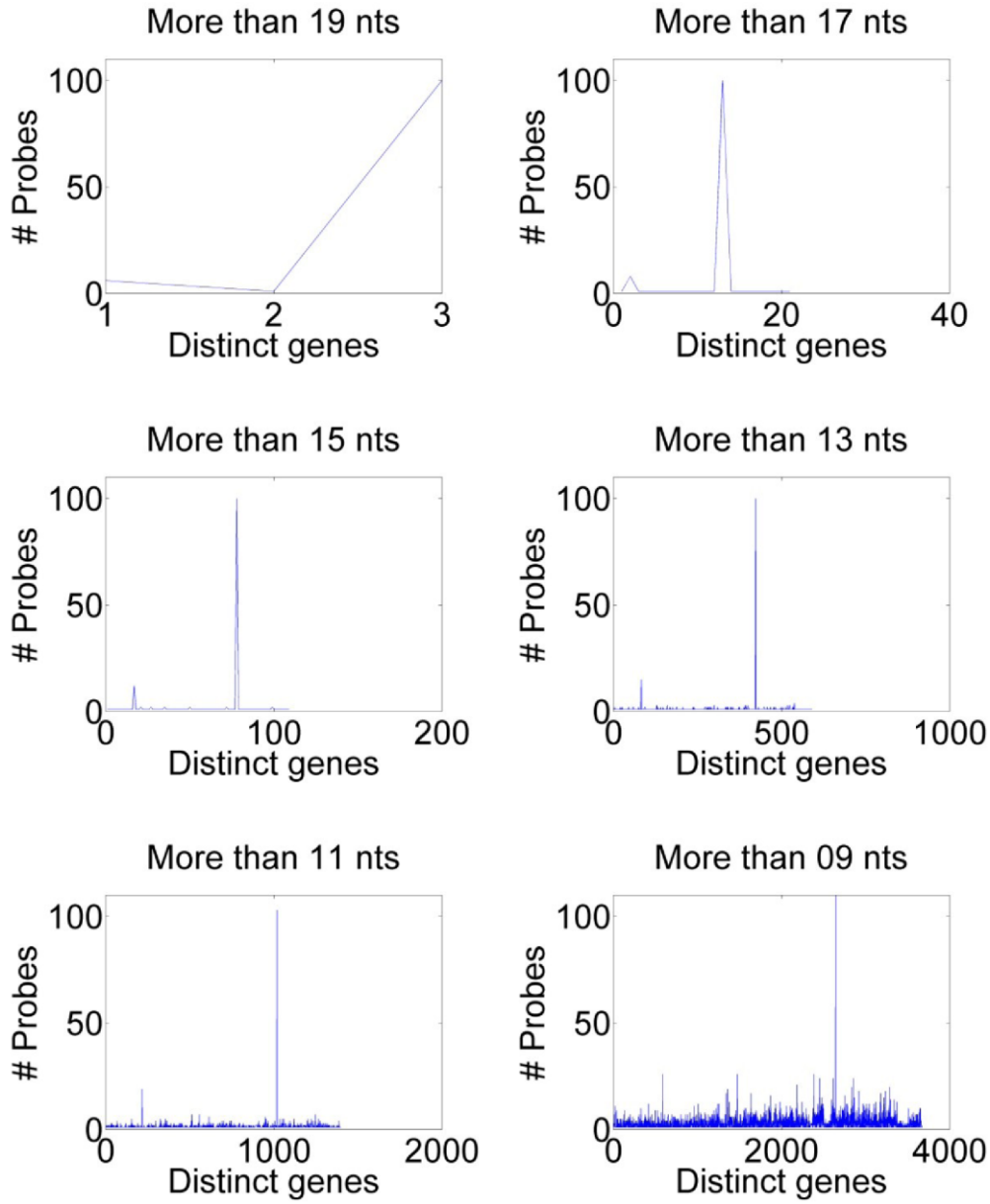

Supplementary Figure S1. Probe design for mRNA FISH. Each *RNR* gene was targeted by 40 20-nucleotide long DNA oligo probes. Each probe was labeled with an Alexa 568 fluorophore through a 3' amine modification. Dual color HPLC was used to purify the fluorophore-conjugated probes following previously described protocols (8, 11). The use of 40 probes per gene ensures that each mRNA single-molecule that is targeted is detectable due to a strong, additive signal even in the presence of some non-specific-binding for any given probe to a different mRNA. But cross-hybridization is of potential concern when genes of high homology are probed, such as *RNR1* and *RNR3* that are nearly 80% identical in nucleotide sequence. (A) The first 180 nucleotides of a sequence alignment of the approximately 2 kb *RNR1* and *RNR3* genes

illustrates their high degree of homology. (B) In order to maintain specificity of the probe designs, 100 probes were initially designed against *RNR1*. Designed probes were interrogated against the yeast genome using a BLAST search. Each graph shows the number of probes that resulted in a "hit" against a particular gene using the threshold value of alignment length indicated. Whereas all 100 probes "hit" *RNR1*, occasionally a probe would also "hit" another gene in the genome. mRNA FISH relies on the fact that the number of these cross-"hits" is few compared with the specific "hit". Because of the high homology between *RNR1* and *RNR3*, specific cross-hits can occur. Even at a threshold value of alignment length greater than 15 or 17 nucleotides (nts), a second peak can be seen. These are the probes designed against *RNR1* that "hit" *RNR3*. Such probes need to be eliminated before synthesizing experimental probes. As the threshold is decreased, additional genes show up as peaks in the graph. This is expected and illustrates why the optimal length of 20 nts was chosen by the original designers of the procedure, namely because at 20 nts cross-hits become increasingly unlikely. Any probe for *RNR1* that showed even a >9nt alignment length with *RNR3* was eliminated. From the remaining probes, 40 were synthesized for experiments. (C) A similar approach was adopted for *RNR3* too. Similar results as in (B) are shown for *RNR3*. The second peak is due to probes that can potentially cross-hybridize with *RNR1*. All such probes were eliminated.

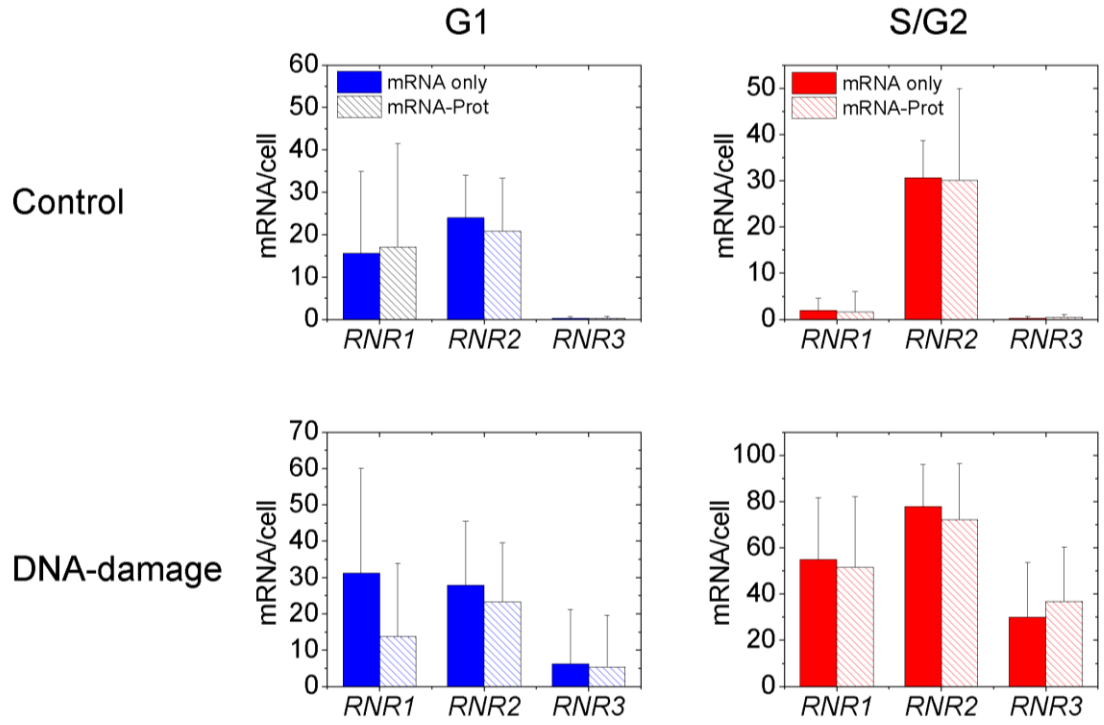

Supplementary Figure S2. Similar mRNA numbers are obtained when mRNA FISH is performed alone or with protein detection. The mean numbers are largely reproduced despite the lower number of cells in the mRNA-Protein experiments. The data is from Figures 2 and 3b. Standard deviations over cells are plotted to show variability among cells. The only pair where the difference looks apparently large (*RNR1* under damage, G1 cells) is not significant at $p<10^{-3}$.

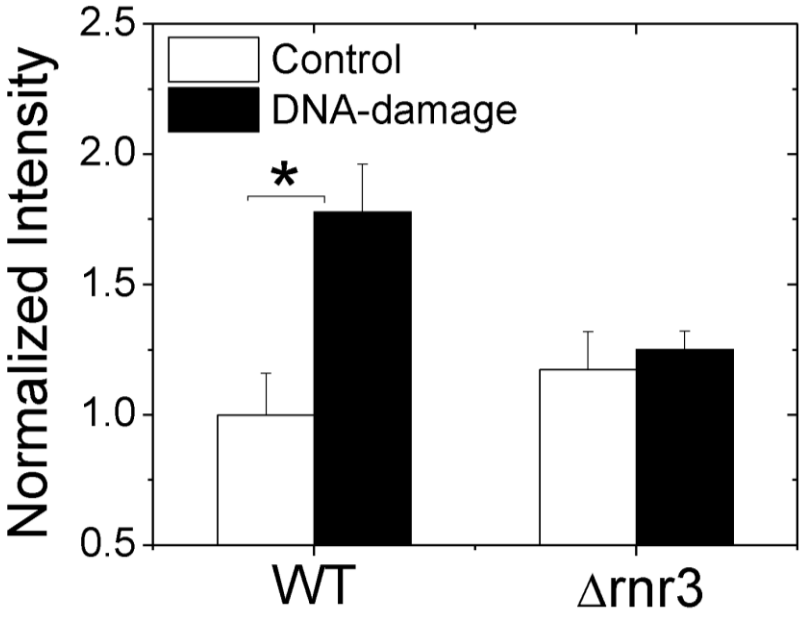

Supplementary Figure S3.The low levels of the Rnr3 antibody staining in control untreated cells which do not express Rnr3 is non-specific. Staining levels are comparable between wildtype (WT) BY4741 and a Δrnr3 strain in the same genetic background. Median intensity values from flow cytometry normalized to the WT control levels are plotted. The error-bars are standard deviations from triplicate measurements on the same day. '*' indicates $p<0.05$ in a Student's t test. There is no significant induction upon DNA-damage by MMS-treatment in the Δrnr3 strain. White bars denote control cells while black bars denote damaged cells.

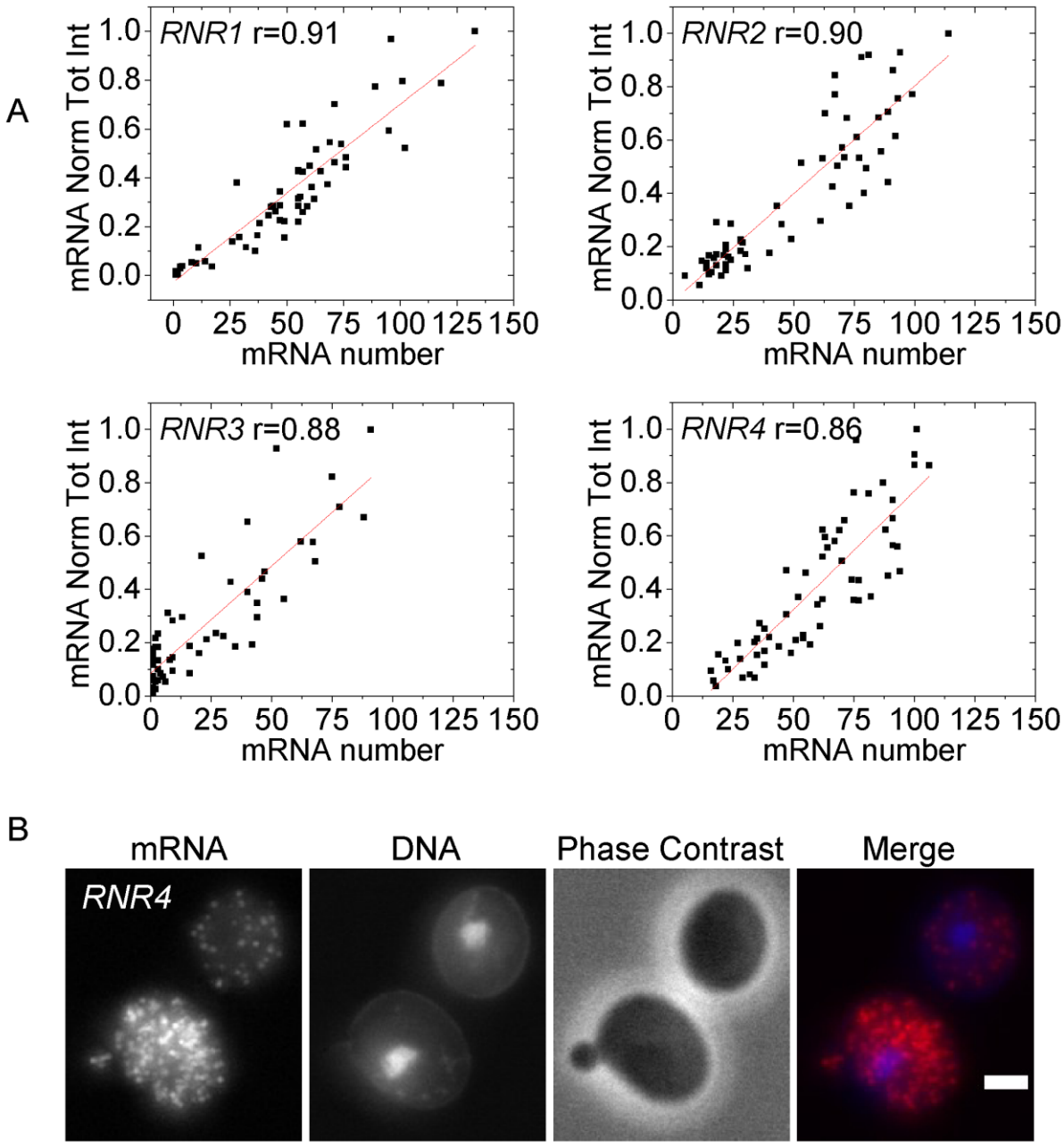

Supplementary Figure S4. (A) RNR genes are highly induced upon DNA damage by MMS. So it is a concern whether the number of mRNA spots within the volume of a cell can be reliably counted as the density of spots increases with MMS treatment, and overlapping fluorescence signals can cause spot numbers to be underestimated. mRNA spots can still be resolved in individual z-planes, however they tend to merge in z-projected images. The spot counting program used by us which was originally developed by Raj et al (8), does not use z-projected images but counts spot signals in 3 dimensions. It has been used to count mRNA spots in yeast

(11). Another work reported that when mRNA spots occur concentrated in one cellular organelle as bright transcription sites, only approximately 40 spots can be counted reliably (9). However, this work showed that autofluorescence-corrected total intensity in the mRNA channel has a linear relationship with mRNA number and this can be extrapolated to find the number of spots when mRNA spots become too dense. This upper threshold of number of mRNA counted reliably, is likely to be higher in our case where mRNA spots are spread throughout the cytoplasm as spatially resolved spots and not concentrated in one organelle. We verified that the program gives very reliable counts when mRNA spot numbers are low, and to be sure that when spots become dense we do not underestimate numbers, we plotted total intensity against mRNA numbers from the program like in the previous study. Indeed throughout the range of the typical range of mRNA numbers measured by us, we saw a linear relationship between mRNA numbers yielded by the program and total intensity of mRNA. The graphs above shows typical plots for all four *RNR* mRNA in cells treated with 0.02% MMS for 1 hour (a typical condition of high mRNA numbers). Data from 60 cells are shown in each case (black squares) and the red-lines represent linear fits. Unlike the mRNA numbers the intensity is not absolute and has been normalized to the maximum intensity value in each case. In every case a linear relationship between mRNA total intensity and count is seen. Pearson's correlation coefficient (r) values are also reported. Because the linear relationship holds throughout the range, and even at the high end we do not seem to be systematically underestimating mRNA numbers, this gives us confidence in the efficacy of the spot counting algorithm in this case. Thus we uniformly used the spot counting algorithm for estimating mRNA numbers in all the instances investigated by us.

(B) A typical image *RNR4* mRNA under conditions of DNA-damage by MMS is shown. Note that the G1 cell on top has relatively fewer transcripts (n=29, by the spot counting algorithm), which are isolated from each other even in a z-projection and can also be counted by hand. However, the S/G2 cell at bottom shows higher induction of *RNR4* mRNA (n=72, by the spot counting algorithm) - individual transcripts cannot be distinguished in a z-projection, but can be counted by the spot-counting algorithm developed by Raj et al (8), and is within the range covered by the graph in (A). The scale-bar shown is 2 μm.

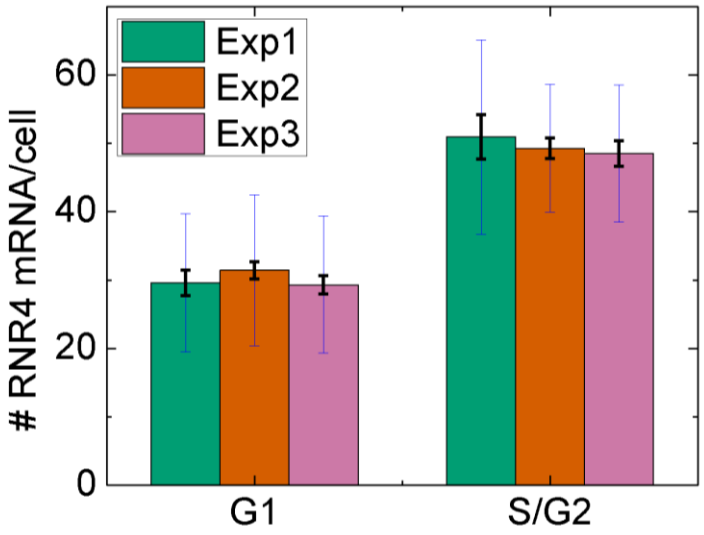

Supplementary Figure S5. Mean numbers are reproducible among different experiments, and variation over cells is much greater than the variation of the means from duplicate experiments. Exp1 (N=47 cells), Exp2 (N=115 cells), Exp3 (N=85 cells) are three experiments done on different days measuring RNR4 mRNA numbers in control cells. Despite the different numbers of cells considered, the mean RNR4 mRNA numbers per cell for G1 and S/G2 cells are remarkably reproducible among the experiments. The error-bars in black are standard-errors, while those in blue are standard deviations over cells. Different replicates of a bulk assay measuring RNR4 mRNA levels will reflect the small variation among the means, but will not capture the heterogeneity among cells. Standard errors as above have been used throughout the manuscript unless otherwise noted. Mean numbers are usually well-determined even in one experiment. Previous single molecule FISH studies (7, 8) have also determined the error over several cells in one experiment, using boot-strapping methods.

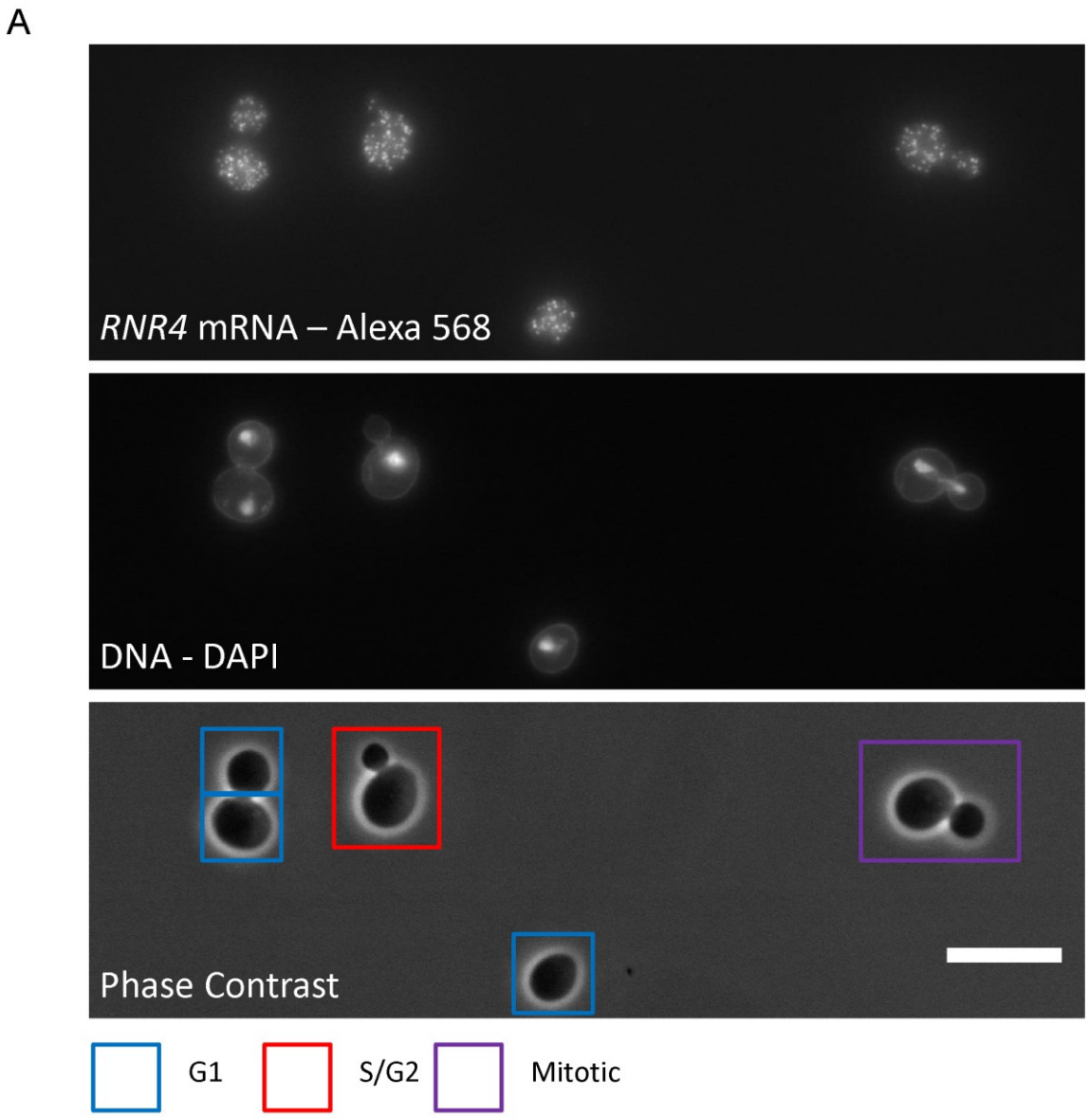

Supplementary Figure S6. Classification of cell-cycle stage. The DAPI and Phase contrast images of isolated cells are used to decide if a cell is in G1 or S/G2 phases according to the presence or absence of a bud and whether complete nuclear division has occurred. Mitotic cells are left out of consideration. Unbudded cells are classified as G1 cells, whereas budded cells which have not undergone nuclear division are classified as S/G2 cells following previous works (1, 2). The scale-bar is 10 μm.

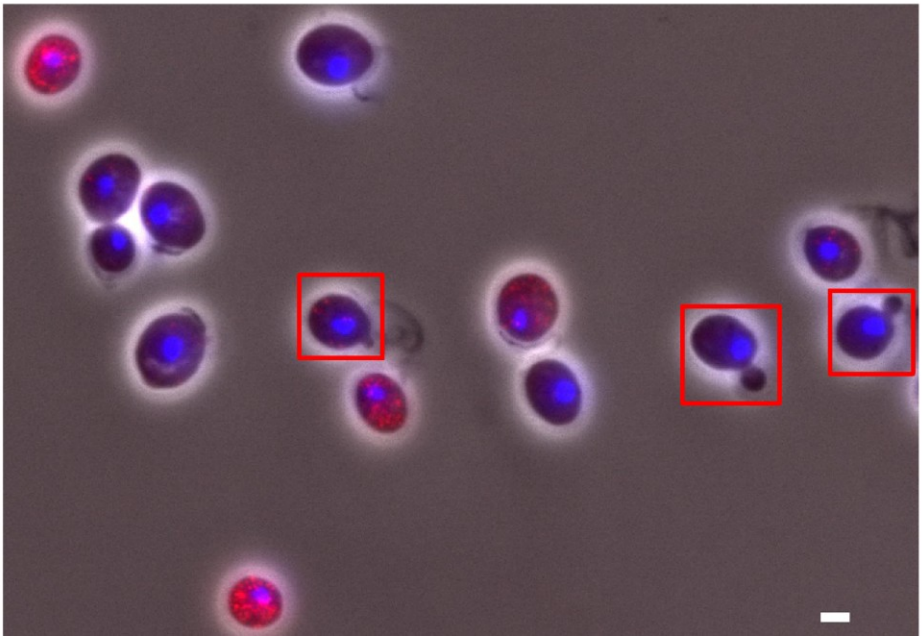

Supplementary Figure S7. FISH is performed for RNR1 mRNA. A field of untreated control WT BY4741 cells is shown. The image is created by merging z-projected mRNA, DNA and phase images. The scale-bar is 2 μm. Red squares mark out the budded S/G2 phase cells.

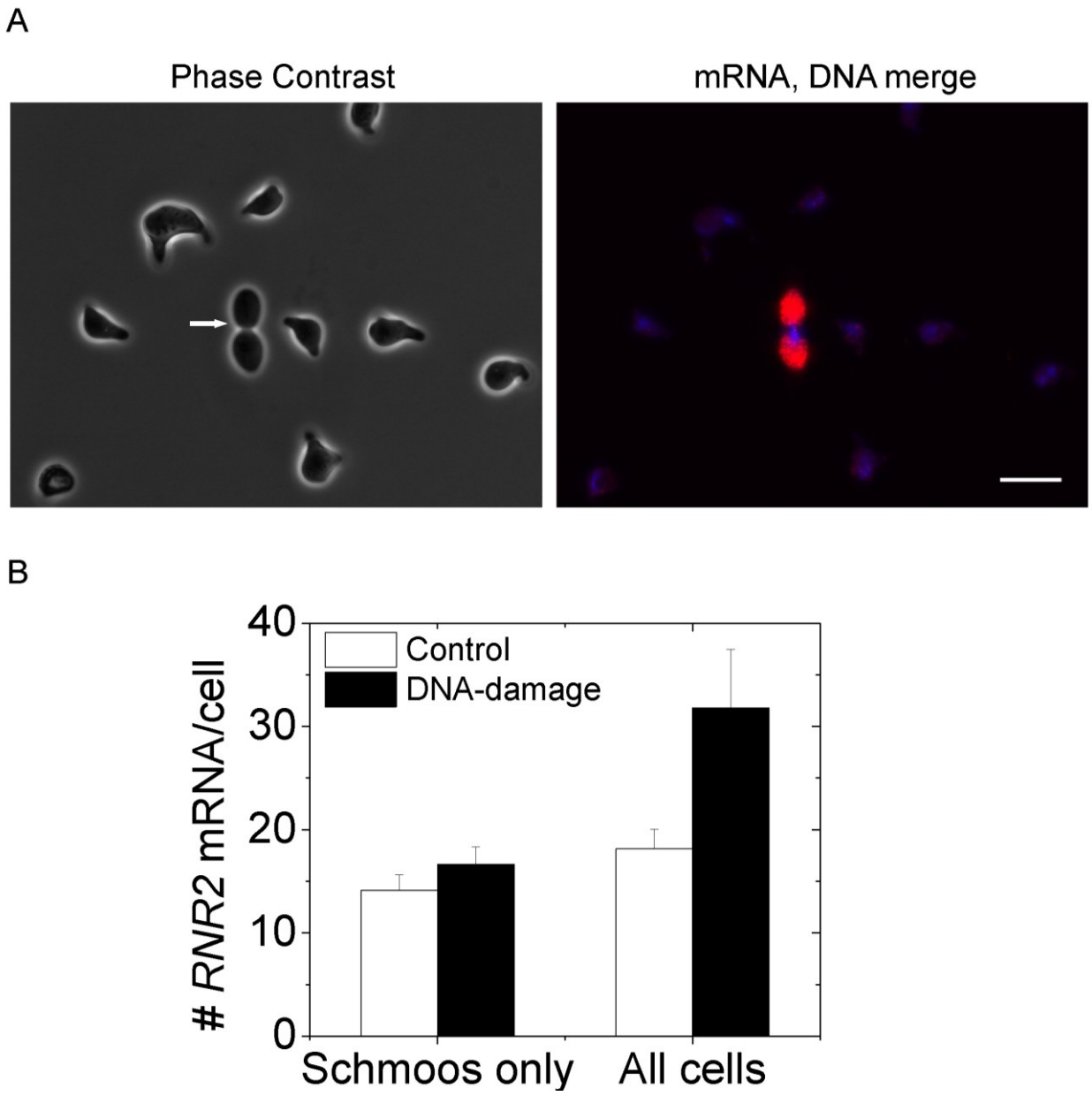

Supplementary Figure S8. (A) RC634 cells were treated with 2 μg/ml α-factor for 2.5 hours and then with 0.01% MMS for 4 hours following previous work (4, 5), and FISH was performed for *RNR2* mRNA. *RNR2* was chosen as it was one of the *RNR* genes which had been shown to be induced in α-factor-arrested cells in the previous works. We found there are always a few escapee S/G2 cells in the culture (see the large budded cell indicated with the arrow which is morphologically distinct from the shmoos). And while ~90% of the cells are still shmoos, the one escapee cell responds dramatically to MMS (*RNR2* mRNA in red and DNA in blue are superimposed). In fact so large is the response that mRNA spot counts are likely to be underestimated due to saturation and merging of transcripts. These cells can bias the mean in a

northern blot. The scale-bar is 10 μm. (B) The mean mRNA numbers are calculated from 70 untreated shmoos and 72 MMS-treated shmoos. White bars denote control cells while black bars denote damaged cells. For the shmoos, the means are 14.1 and 16.6 – essentially the same. Now the large budded cells were added to the calculation – taking the total number of cells to 79 untreated and 80 treated. However, with this modest increase in cell numbers, a clear difference in the means was created. While not significant at $p< 10^{-3}$ in a KS test due to the huge difference in numbers (the 8 MMS-treated escapee cells have very large mRNA numbers ranging from 100 to 285, with a mean of ~168 mRNA; in contrast, the mean mRNA number is only 16.6 in the 72 shmoos), the difference is likely to show in an assay which measures only the mean. Also note that, in fact, mRNA counts are underestimated in the escapee cells. Importantly, the shmoos show no *RNR2* induction. Thus *RNR* induction is indeed lower in true G1 cells.

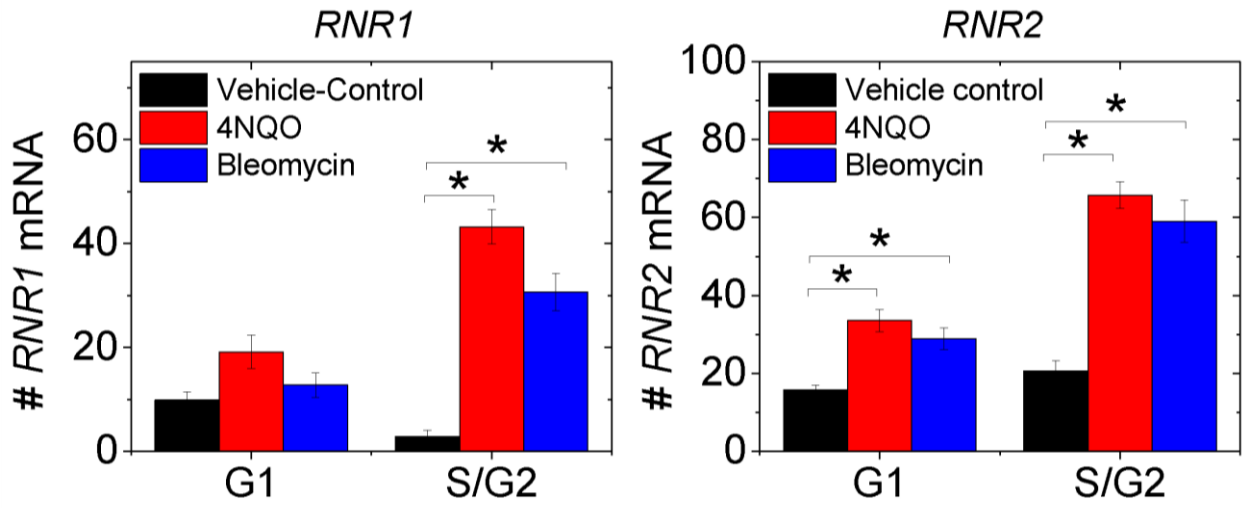

Supplementary Figure S9. *RNR* response to 4-NQO and bleomycin. WT BY4741 cells were either mock-treated with vehicle, or treated either with 4-NQO (0.25 μg/ml, 1 hr) or bleomycin (2.5 μg/ml, 1 hr), and FISH was performed for *RNR1* and *RNR2* in separate samples. In both cases the relative induction is larger in S/G2 cells. At least 50 cells were counted for each experiment. '*' implies $p<10^{-3}$ in a KS test.

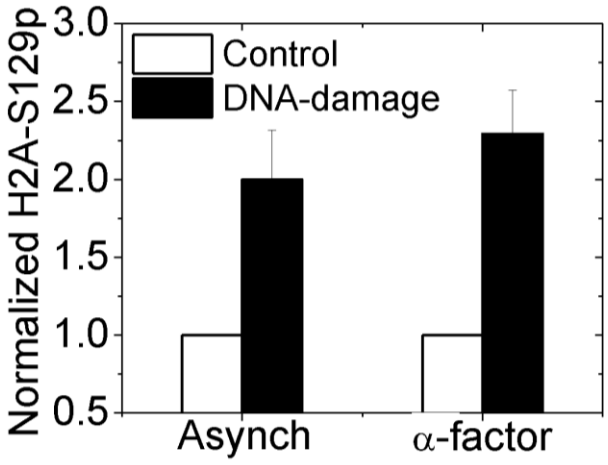

Supplementary Figure S10. Induction of phosphorylated H2A-S129 (H2A-S129p) upon DNA-damage by 0.02% MMS for 1 hour measured by flow cytometry. Asynchronous and α-factor (5 μg/ml, 3 hours) arrested BY4741 cells were subjected to DNA-damage by 0.02% MMS for 1 hour. Cells were fixed and antibody staining was performed as described in the methods section with a primary antibody against H2A-S129p. An Alexa-488 conjugated secondary antibody was used. All experiments are normalized with respect to the control untreated samples that have a value of 1 for normalized H2A-S129p intensity. Each experiment was performed three times on different days. The error-bars are standard deviations of the three mean relative inductions thus obtained. In principle α-factor arrested cells should be compared to G1 cells in an asynchronous population, but cell-cycle stage is not resolved in these experiments. But the α-factor arrested cells show the same relative induction as an asynchronous population averaged across the all cell-cycle stages. While this induction is relative, and absolute protein levels cannot be deduced, we note this may indicate that α-factor arrested cells activate checkpoints differently from G1 cells in a cycling population, as no activation of H2A-S129 phosphorylation is seen in the bulk of the G1 cells in asynchronous cultures (Figure 5).

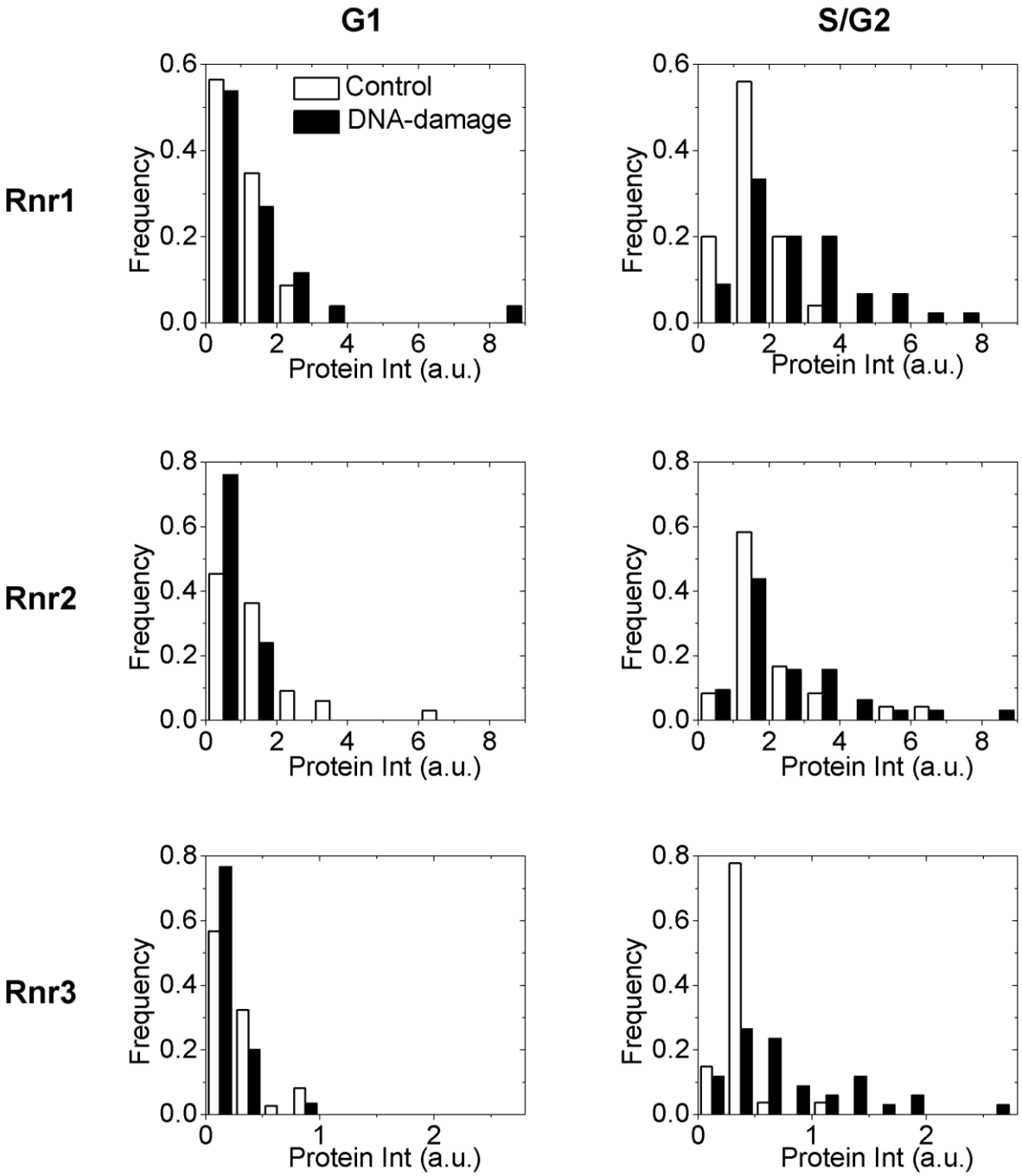

Supplementary Figure S11. Protein histograms for the studied RNR genes. White bars denote control cells while black bars denote damaged cells. Bear in mind that the Rnr3 protein is not present in the absence of damage.

References

1. **Berger, A. B., G. G. Cabal, E. Fabre, T. Duong, H. Buc, U. Nehrbass, J. C. Olivo-Marin, O. Gadal, and C. Zimmer.** 2008. High-resolution statistical mapping reveals gene territories in live yeast. Nat Methods **5:**1031-1037.
2. **Calvert, M. E., J. A. Lannigan, and L. F. Pemberton.** 2008. Optimization of yeast cell cycle analysis and morphological characterization by multispectral imaging flow cytometry. Cytometry A **73:**825-833.
3. **Day, A., C. Schneider, and B. L. Schneider.** 2004. Yeast cell synchronization. Methods Mol Biol **241:**55-76.
4. **Elledge, S. J., and R. W. Davis.** 1989. DNA damage induction of ribonucleotide reductase. Mol Cell Biol **9:**4932-4940.
5. **Elledge, S. J., and R. W. Davis.** 1990. Two genes differentially regulated in the cell cycle and by DNA-damaging agents encode alternative regulatory subunits of ribonucleotide reductase. Genes Dev **4:**740-751.
6. **Haase, S. B., and S. I. Reed.** 2002. Improved flow cytometric analysis of the budding yeast cell cycle. Cell Cycle **1:**132-136.
7. **Raj, A., C. S. Peskin, D. Tranchina, D. Y. Vargas, and S. Tyagi.** 2006. Stochastic mRNA synthesis in mammalian cells. PLoS Biol **4:**e309.
8. **Raj, A., P. van den Bogaard, S. A. Rifkin, A. van Oudenaarden, and S. Tyagi.** 2008. Imaging individual mRNA molecules using multiple singly labeled probes. Nat Methods **5:**877-879.
9. **Tan, R. Z., and A. van Oudenaarden.** 2010. Transcript counting in single cells reveals dynamics of rDNA transcription. Mol Syst Biol **6:**358.
10. **Taniguchi, Y., P. J. Choi, G. W. Li, H. Chen, M. Babu, J. Hearn, A. Emili, and X. S. Xie.** 2010. Quantifying E. coli proteome and transcriptome with single-molecule sensitivity in single cells. Science **329:**533-538.
11. **Youk, H., A. Raj, and A. van Oudenaarden.** 2010. Imaging single mRNA molecules in yeast. Methods Enzymol **470:**429-446.